Journal of Materials Processing Tech. 299 (2022) 117320

Contents lists available at ScienceDirect

Journal of Materials Processing Tech.

journal homepage: www.elsevier.com/locate/jmatprotec

Suppression of diamond tool wear with sub-millisecond oxidation in ultrasonic vibration cutting of steel

Xinquan Zhang [a], Rui Huang [b,*], Yang Wang [c], Kui Liu [b], Hui Deng [d], Dennis Wee Keong Neo [b,*]

[a] School of Mechanical Engineering, Shanghai Jiao Tong University, 800 Dongchuan Road, Shanghai 200240, China
[b] Singapore Institute of Manufacturing Technology, 73 Nanyang Drive, 637662, Singapore
[c] College of Mechanical and Electrical Engineering, Nanjing University of Aeronautics and Astronautics, Nanjing 210016, China
[d] Department of Mechanical and Energy Engineering, Southern University of Science and Technology, No. 1088, Xueyuan Road, Shenzhen, Guangdong 518055, China

ARTICLE INFO

Associate Editor: Erhan Budak

Keywords:
Coolant air blowing
Chemical tool wear
Diamond
Ultrasonic vibration cutting
Oxidation

ABSTRACT

Ultrasonic vibration has been applied to suppress the chemical tool wear in ultra-precision diamond cutting of steel and other alloys. The tool wear is found significantly reduced with enriched ambient oxygen concentration. In this study, instead of supplying costly and potentially hazardous high concentration oxygen to the machining zone, a greener alternative, high-pressure air coolant has been applied to enhance the oxygen content at the cutting area. The effect of air-blowing pressure on ultrasonic vibration cutting of stainless steel was investigated, using both polycrystalline and single-crystal diamond tools. It has been found that an increased air blowing pressure and a more closely positioned nozzle not only improve the cutting performance but also reduce tool wear, reflecting consequences from both chemical and fluidic dynamics aspects. A higher air blowing pressure will increase the instantaneous air pressure as well as the density of oxygen molecules around the cutting zone. This increases the passivation speed for the freshly cut steel surface caused by the formation of thin oxide layers. Experimental results have formalized the findings that sub-millisecond oxide formation is the key factor to suppress diamond tool wear.

1. Introduction

Diamond turning is widely used in the optics manufacturing industry to produce optics components and molds made of plastics or metal alloys, owing to its superior surface finish and form accuracy generated. Unfortunately, only a handful of types of metallic alloys (Aluminum, Copper, etc.) can be directly cut using diamond tools with acceptable tool life. Various common metal alloys cannot be directly cut using diamond (Steel, Nickel, Tungsten, etc.) due to the strong chemical affinity between these alloys and diamond. Paul et al. (1996) studied the chemical tool wear in diamond turning and have identified that this chemical affinity between diamond and the non-diamond-turnable metals is caused by the unpaired *d*-shell electrons of the metal element. Iron is the most widely used engineering metal element and has 4 unpaired *d*-shell electrons.

To implement steel as the mold material, the manufacturers usually coat a physical layer made of nickel-phosphorus alloy on a steel substrate before cutting this diamond-turnable layer. Unfortunately, the nickel alloy starts recrystallizing when the temperature is above 400 °C, and its mold life is also much less than steel. To directly cut the steel using a diamond without any additional plating, two major alternative methods, ultrasonic vibration cutting (UVC) and surface nitriding were invented by Shamoto and Moriwaki (1999) and Brinksmeier and Gläbe (2002). Compared to surface nitriding, UVC shows more promising results and has been industrially adopted for injection molding of plastic optical components with non-nickel-plated steel molds. The suppressing mechanism of diamond tool wear in UVC has been unclear in the past decades, causing limited advancement and its adoption in the industry. Both Zhang et al. (2019) and Fukumori et al. (2019) have demonstrated that an enhanced oxide formation around the cutting zone suppresses chemical wear in UVC. The diamond tool wear is suppressed by 70 % in an oxygen-shielded environment when cutting stainless steel. However, maintaining the oxygen shielding is costly and can pose a potential fire hazard due to the extremely high oxygen concentration. To have a safer and more convenient alternative, a high-pressure air coolant is used in this study to achieve tool wear suppression through a more affordable and sustainable approach.

To ensure the tool's complete separation from the cutting zone, the resultant linear speed of the tool against the workpiece should be kept

* Corresponding authors.
E-mail address: huang_rui@simtech.a-star.edu.sg (R. Huang).

https://doi.org/10.1016/j.jmatprotec.2021.117320
Received 24 March 2021; Received in revised form 16 July 2021; Accepted 7 August 2021
Available online 12 August 2021

Nomenclature

x	Displacement in the X direction
y	Displacement in the Y direction
t	Time
f	Vibration frequency
v_c	Relative tool-workpiece speed, i.e. Nominal cutting speed
a	Vibration amplitudes along the cutting direction
b	Vibration amplitudes along the thrust direction
$\varnothing$	Phase shift
f_r	Feed rate
A_p	Depth of cut
v	Flow speed
p	Fluidic pressure
ρ	The density of the gas
Ψ	Potential associated with the conservative force field
$\mathbf{A}\mathbf{e}^{-\frac{E}{RT}}$	A coefficient for reaction rate
P	The partial pressure of gas element
γ	Increase of the free activation energy
PSI	pounds per square inch
Pa	Pascal

smaller than the maximum vibrating speed of the ultrasonic motion, therefore limiting the maximum cutting speed. Amongst the research published related to diamond tool wear reduction in UVC, three major hypotheses for the tool wear suppression are summarized: 1) Reduction of cutting temperature due to enhanced cooling around the vibration gap by Brehl and Dow (2008), 2) Reduction of contact time due to the consistent tool-workpiece separation by Zhang et al. (2014), and 3) Formation of inert thin-film oxide on the freshly cut steel surface by Brinksmeier et al. (2006). All three hypotheses clearly explain the two common phenomena in UVC: 1) a lower cutting speed generally resulted in reduced tool wear, and 2) two-dimensional (2D) UVC leads to less tool wear than one-dimensional (1D) UVC. The difference between 1D and 2D UVC is detailed in Section 2.1. As a lower cutting speed will lead to a lower cutting force, shorter engagement time as well as the longer exposure time of the freshly cut steel to the atmosphere, it will eventually result in a lower cutting temperature, shorter contact time for the chemical reaction between C and Fe as well as thicker iron oxide on the freshly machined workpiece, respectively. Moreover, as 2D UVC will lead to a lower cutting force due to the reversed tool-chip frictions well as a larger physical gap between the diamond tool tip and workpiece, it will also pose a more positive effect on the diamond tool wear suppression compared to 1D UVC.

In the conventional turning, milling, and grinding process, high-pressure flood coolant has been well established and implemented by the industry to realize a deeper penetration of metalworking fluids into the contact zone, to improve its cooling and lubricating function and eventually the cutter tool life. Although UVC has already been applied in the machining of steel for several decades since the development of the UVC device by Moriwaki and Shamoto (1991), there is no research studying the effect of coolant air on the tool wear condition and the cutting performance. As the ultrasonic vibration creates a regular separation between the tool and workpiece, it is expected that high-pressure air blowing may also pose a positive effect on suppressing the tool wear in UVC of difficult-to-cut materials. Cong et al. (2011) has utilized cool air in a rotary ultrasonic vibration machining of composite materials to improve the cutting performance. More importantly, the variation of coolant air condition will not affect the tool-workpiece contact time of the UVC process, but only possibly affect the cutting temperature and the formation of iron oxide. Hence, it is necessary to conduct experiments to investigate and understand the effect of coolant air blowing pressure on the tool wear suppression mechanism, and also provide guidance to engineers for further improving the diamond tool life.

In this paper, experiments have been conducted to study the air blowing pressure on the cutting performance in these aspects (1) tool wear, (2) surface roughness, and (3) cutting force, in UVC of steel. It has been found that an appropriately higher supplying air pressure would generally lead to reduced diamond tool wear and better cutting performance, possibly due to the increased passivation speed for the freshly machined steel surface caused by the formation of a thin oxide layer. A preliminary calculation has revealed that more than one layer of iron oxide can grow within a UVC cycle. In practice, this study may serve as a guideline to suppress diamond tool wear when more cleanly and affordably when cutting non-diamond-turnable metals, such as steel.

2. Method and experimental setups

2.1. Ultrasonic vibration cutting

There are two common types of ultrasonic vibration cutting processes: 1D UVC and 2D UVC. Fig. 1 shows a schematic of a typical 2D UVC process, elliptical vibration cutting, at an operating frequency of 38.9 kHz. Its tool-workpiece position with respect to time (t) can be given as follows:

$$\begin{cases} x(t) = a\cos(2\pi ft) - v_c t \\ y(t) = b\cos(2\pi ft + \varphi) \end{cases} \quad (1)$$

where f is the vibration frequency, the relative tool-workpiece speed is v_c, a and b are vibration amplitudes along the cutting direction and thrust direction, respectively, and $\varnothing$ is phase shift and usually set 90 ° in most 2D UVC processes. 1D UVC can be considered as a special 2D UVC process with no vertical vibration or the vibration amplitude along the thrust direction is zero (i.e. $b = 0$).

To realize intermittent cutting in UVC of a workpiece, there is a threshold value of maximum cutting speed (i.e. $2\pi af$), summarized by Brehl and Dow (2008). It is necessary to set the cutting speed below such value to ensure that the tool can be separated from the workpiece material during vibration. Otherwise, continuous cutting without any tool-workpiece separation will occur even the vibration motion is applied on the cutting tool, and there will be little improvement on the cutting performance compared to conventional cutting.

2.2. Experimental setup using polycrystalline diamond tools

The UVC tests are conducted using polycrystalline diamond (PCD) tools manufactured by *Sumitomo*. The workpiece is made of hardened stainless steel (*STAVAX*), which is provided by *ASSAB* and widely used as the mold material for injection molding of optical components. During the experiments, a UVC system generates 2D elliptical vibration with 4 μm peak-to-peak amplitudes on both cutting and thrust directions, as shown in Fig. 2(a). Each face cutting test starts from the workpiece edge, 40 mm diameter, and ends at 28 mm diameter, with a cutting distance of 200 m approximately, as shown in Fig. 2(b). Dry air alone with 20 °C temperature is utilized in all the tests without oil or any other coolant media included.

Conventionally, there are two major functions of coolant air supplied to the cutting process: 1) blowing away the chips, and 2) assisting to form spray mist. There is no specific requirement for the pressure of air blowing in ultra-precision machining because even a very low-pressure air blowing is sufficient to produce the mist and blow away the chips, which are usually very tiny and light. In general, the heat generated in the cutting process is taken away by the mist which contacts the tool and workpiece through conduction and evaporation. Compared to mist, air coolant dissipates heat via convection and hence plays a less important role in lowering the temperature of the tool and workpiece. It is necessary to note that, in practice, the commonly utilized air blowing pressure

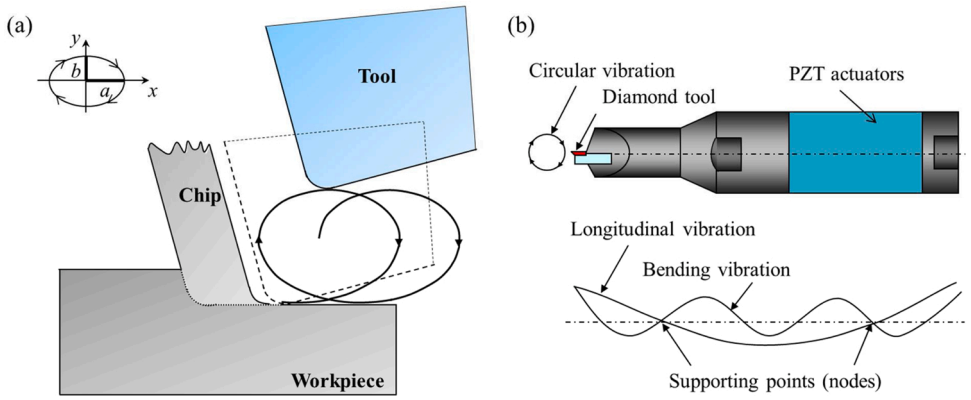

Fig. 1. (a) Schematic view for the elliptical vibration cutting process; and (b) a 2D ultrasonic vibrator and its vibration modes, by Suzuki et al. (2007).

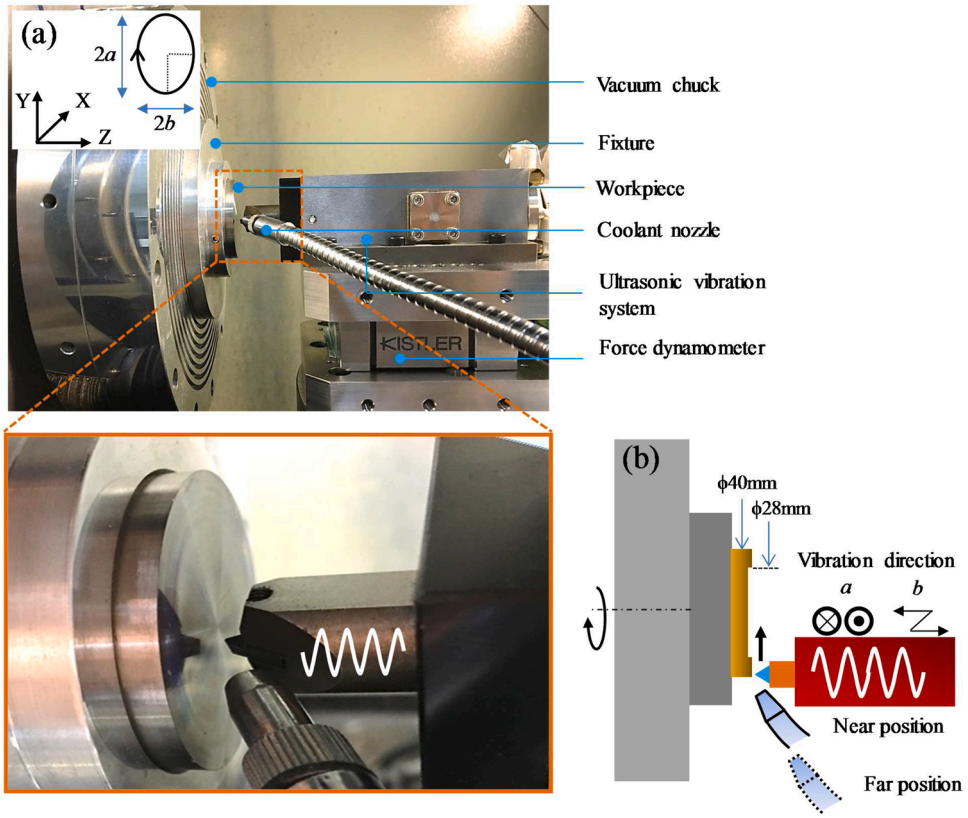

Fig. 2. (a) Experimental setup of the UVC tests on an ultra-precision machining system (Moore Nanotech 350 F G); and (b) schematic illustration of the experimental setup with the indication of different nozzle locations.

in ultra-precision machining for mist coolant in diamond turning is < 20 PSI, i.e. $< 1.38 \times 10^5$ Pa, finishing cut is done to the fact that a large pressure with strong turbulent airflow may cause unwanted tool vibration and chattering marks on the workpiece.

In this study, cutting tests using PCD tools are conducted under four different air-blowing pressure conditions, and a total cutting distance of 800 m has been reached through four rounds of 200 m cutting, for each tool. Furthermore, as the gas density and instant pressure of blowing air quickly drops once the air is ejected out from the nozzle, two different relative locations of the nozzle to the tooltip are studied to investigate its effect on tool wear and cutting performance, because it is considered that different nozzle locations may give different pressure and velocity distribution of the air. To precisely understand the effect of the coolant air on the tool-work interface, Computational Fluid Dynamics (CFD) simulation is conducted in Section 3 to identify the effective pressure on the work-tool interface under different conditions.

Hence, 32 rounds of cutting tests in total are conducted using 8 PCD tools to evaluate and compare the tool wear progression and cutting performance in this study. Table 1 lists the conditions and parameters used for the UVC cutting tests. To ensure consistency of the unit, Pa will be used in this manuscript instead of PSI.

3. Simulation modeling and theoretical analysis

To precisely and quantitatively understand the effect of the coolant air on the tool-work interface, CFD simulation is first conducted to understand and compare the capability of air penetration into the tool-workpiece gap created by the ultrasonic vibration, using *Ansys Fluent 18.2*. The simulation identifies the crucial parameters for understanding the effect of the blowing air onto the tool-work interface during a UVC

Table 1
Cutting conditions for UVC of hardened stainless steel using PCD tools.

Parameters			Values			
Cutting condition	Feed rate, f_r (μm/rev)		3			
	Depth of cut, A_p (μm)		5			
	Spindle rotation rate, (RPM)		20			
	Nominal cutting speed, v_c (m/min)		2.637 ~ 3.768			
	Time for each cutting round (mins)		67			
Vibration condition	Tangential amplitude, a (μm)		2			
	Vertical amplitude, b (μm)		2			
	Vibration frequency, kHz		38.9			
Workpiece condition	Cutting zone dimensions (mm)	Outer diameter	40			
		Inner diameter	28			
	Material		STAVAX (13.6 % Cr, 84 % steel, 2.4 % others)			
	Hardness		49 HRC			
Coolant condition	Coolant media		Dry air			
	Supplying air pressure	PSI	20	40	80	100
		10^5 Pa	1.38	2.76	5.52	6.89
	Nozzle outlet inner diameter		1 mm			
	Distance from nozzle outlet to the tooltip	Near position	≈ 10 mm			
		Far position	≈ 20 mm			
Cutting tool	Tool material		PCD (DA1000)			
	Grain size		≤ 0.5 μm			
	Nose radius (mm)		0.2			
	Rake angle (°)		0			
	Clearance angle (°)		11			

cycle, namely: 1) whether the air can reach the tool-work interface within the ultrasonic cycle at a given frequency (38.9k Hz in this study), and 2) the acting partial pressure of oxygen on the tool-work interface at different supplying pressure and nozzle distance.

The finite element models (FEM) were deployed to help understand the fluidic dynamics at the machining area. However, due to the complexity of the cutting configurations, the FEM was performed in two steps. The first model is designed to determine the theoretical fluidic velocity, considering the position of the nozzle in the system and the supplying pressure of the air coolant. Its configuration is shown in Fig. 3 (a), (b), based on the cutting conditions in Table 1.

The air bounded between the tool post and the workpiece is meshed for CFD analysis, and it is marked green in Fig. 3. The velocities under different conditions are obtained at the tooltip position, indicated in Fig. 3(b).

After obtaining the fluid velocities at the cutting area in the first model are used as the input to simulate the air pressure between the tool rake face and the chip, i.e. the acting pressure of the micrometric machining zone. As shown in Fig. 4, the boundary conditions are illustrated and cutting parameters following Table 1, the distance between the tool and the chip is the tool vibration amplitude (2 μm). The tool-chip configuration is simplified from the study by Shamoto and Moriwaki (1994).

Some assumptions are made in this simulation: (1) The 2D simulation is used with the configuration illustrated in Figs. 3 and 4, (2) The flow is turbulent throughout the process, (3) the kinetic energy does not dissipate to the walls and (4) the air velocity is constant across the inlet, as illustrated in Fig. 4.

3.1. CFD simulation of the fluid velocity at the cutting area

In this dynamic model, compressed air is sprayed from the right bottom of the configuration, to simulate the actual conditions shown in Section 2. Bernoulli's principle indicates that the flow speed of a fluid increases when the flow is narrowed in an incompressible flow. While for a compressible gas under the action of conservative forces, the flow can be described by Clarke et al. (2007) that:

$$\frac{v^2}{2} + \int_{p1}^{p} \frac{d\tilde{p}}{\rho(\tilde{p})} + \Psi = C \tag{2}$$

Where v is the flow speed, p is the pressure and ρ is the density of the gas, Ψ is the potential associated with the conservative force field.

The CFD results are shown in Fig. 5. When the nozzle is near, i.e. 10 mm away, the fluid velocities at the cutting zone are at 150, 350, 500, and 650 m/s, for supplying pressures of 1.38×10^5, 2.76×10^5, 5.52×10^5 and 6.89×10^5 Pa, respectively. While at the far position of 20 mm, the corresponding fluid velocities are 70, 300, 400, and 450 m/s, respectively. It is observed that the velocity of compressed air is higher when the nozzle is near the cutting zone and increases with higher supplying pressure.

3.2. CFD simulation of the air pressure at the tooltip

Using the FEM model discussed, the acting pressure at the tooltip could be evaluated. The simulated results are presented in Fig. 6. It is observed that 1) the supplying air will penetrate into the small gap between the cutting tool and the workpiece, 2) the acting pressure of the air coolant increases with the supplying pressure, and 3) the acting pressure is higher when the nozzle is closer to the cutting zone. As the nozzle supplying pressure increases from 1.38×10^5 Pa to 6.89×10^5 Pa, the air pressure between the tool and the chip increases from 1.78×10^5 Pa to 13.1×10^5 Pa (Fig. 6(a)–(d)) when the nozzle is near, and from

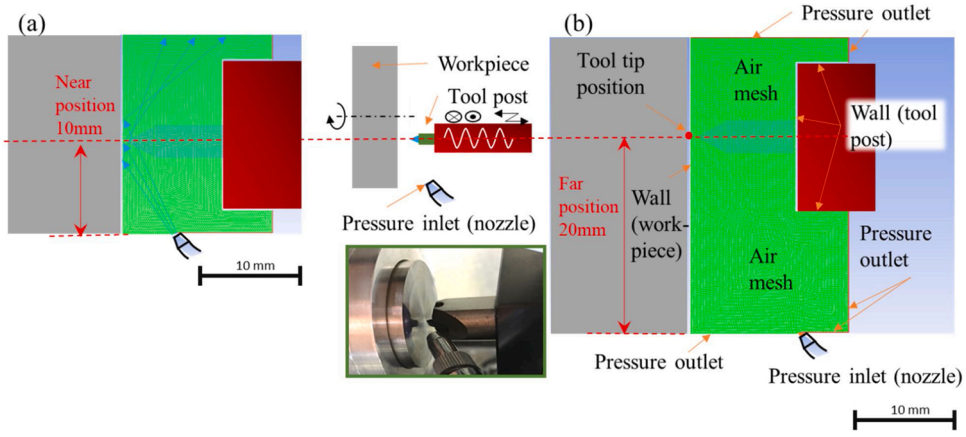

Fig. 3. FEM configuration of the 2D tool-work area with the nozzle at (a) near position, (b) far position. (For interpretation of the references to colour in this figure text, the reader is referred to the web version of this article.)

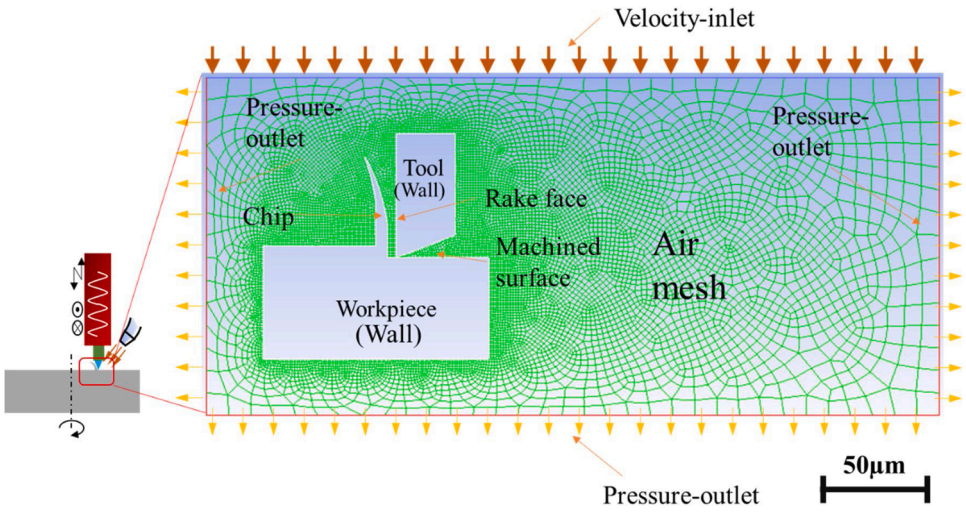

Fig. 4. CFD finite element model to simulate the air pressure between the tool and the chip.

1.17×10^5 Pa to 7.86×10^5 Pa (Fig. 6(e)–(h)) when the nozzle is 20 mm from the cutting zone. The trend is very similar to that in Fig. 5(b), indicating a high correlation between the flowing speed and the acting pressure. Nevertheless, though the practical fluid dynamics might not be as ideal, the trend remains unchanged.

3.3. Theoretical tool wear suppression mechanism of UVC with high oxygen concentration

Generally, diamond is considered stable at room temperature for its high kinetic energy required to oxidize its carbon atoms in gaseous oxygen. On the contrary, most metals are more reactive and a thin layer of metal oxide will form on its surface once exposed to oxygen, such as iron or aluminum. The formation of such oxide starts from the initial adsorption of molecular oxygen and its subsequent dissociation from molecule into chemisorbed atomic oxygen and forms covalent bonds with metal atoms subsequently. The metallic oxide thickness will grow over time until it is too thick to allow subsequent electron emissions. The thickness of oxide can be derived from a logarithmic model by Eley and Wilkinson (1960).

$$\frac{dg}{dt} = Ae^{-\frac{E}{RT}} \times P^{0.6} \times e^{-\frac{\gamma s}{RT}} \tag{3}$$

Where g is the thickness of oxide, t is time, $Ae^{-\frac{E}{RT}}$ is a coefficient for reaction rate, P is the partial pressure of Oxygen, and γ is the increase of the free activation energy.

To verify the relationship between the oxygen concentration and the metal oxide formation, a study was conducted, using an X-ray photoelectron spectroscopy (XPS) developed in-house. An iron workpiece of 1 mm thickness is polished to surface roughness $Ra < 4$ nm, and loaded into the XPS reaction chamber. The iron workpiece is allowed to oxidize in three pure oxygen pressures for the same period. To ensure the starting surface is identical in each round of experiments, argon-ion is sputtered onto the surface to remove any remaining iron oxide from previous experiments.

The iron workpiece was exposed at 0.004 Pa, 0.04 Pa and 0.4 Pa, respectively. The average oxide thickness measured after 1000 s is 2.4 nm, 3.0 and 3.2 nm, as shown in Fig. 7(b). By substituting the measured thickness results, the oxide growth rate could be derived from Eq. (3), which shows a logarithmic relationship between the growth rate and the existing oxide thickness.

For a higher air blowing pressure, the instantaneous air pressure around the cutting edge is increased accordingly. According to the relationship between air density and pressure, higher air pressure will lead to more air molecules (including oxygen molecules) around the vibration gap:

$$\rho = \frac{p}{RT} \tag{4}$$

where ρ is the density, p is absolute pressure, R is the specific gas constant air, and T is the absolute temperature. A higher density of oxygen molecules leads to a higher oxide generation speed thus a thicker iron oxide within a certain period. The oxide thicknesses under different experimental conditions are plotted in Fig. 8. It can be observed that the oxide layer thickness increases with the acting air pressure, thus the partial pressure of Oxygen gas increases. Therefore, within the time for one ultrasonic vibration cycle, a thicker and more complete oxide layer will suppress significantly the diamond tool wear caused by the catalytic effect of the iron atoms.

The operating UVC cycle time is 1 / 38.9 Hz = 2.5×10^{-5} s. The theoretical oxide thickness can then be calculated based on these submillisecond cutting intervals. Fig. 8(a) shows the oxide growth rate at three conditions, which are: (1) without supplying air (1.01×10^5 Pa), (2) highest acting air pressure at far position, 7.8×10^5 Pa (the experimental condition in Fig. 6d) and (3) highest supplying air pressure at far position, 13.1×10^5 Pa (the experiment condition in Fig. 6h). The values are calculated based on the acting pressures derived from Fig. 6.

The details of the calculated grown oxide layer thickness are described in Table 2 and plotted in Fig. 8(b). The number of molecular layers of iron oxide increases thus reducing the chances of free iron atoms from catalyzing the chemical reaction at the diamond tool edge. As the thickness of oxide increases, the tool wear suppression mechanism also gradually saturates towards an equilibrium threshold.

4. Results of polycrystalline diamond tool wear

Every PCD tool is taken out from the tool holder for tool wear investigation using a microscope for every 200 m cutting distance, i.e. one cutting round. The PCD tool is then put back on the tool holder at the same location, and 4 sets of investigations are conducted for each PCD tool used for the 4 rounds of cutting. The air blowing condition and nozzle location are kept unvaried for each tool.

Fig. 9(a) shows the microscopic images of worn tool flank face after 800 m cutting distance for both the near and far position air blowing, and Fig. 9(b) shows the averaged tool flank wear (VB) of these two air blowing conditions against the supplying air blowing pressure. It can be observed that an increased air blowing pressure generally leads to a decreased tool flank wear, for both near and far positions of the coolant nozzle.

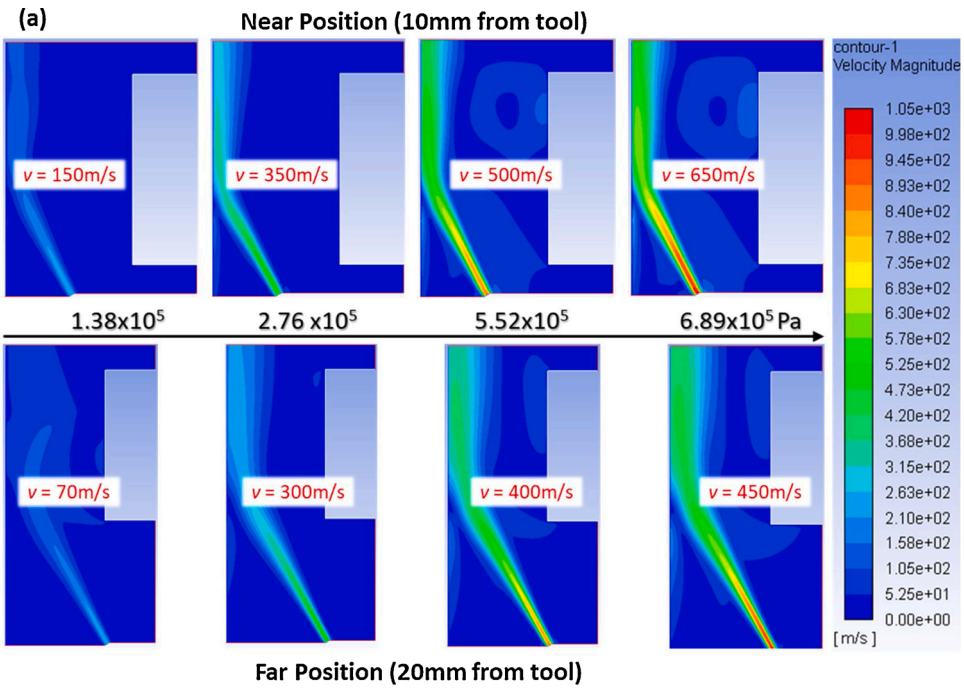

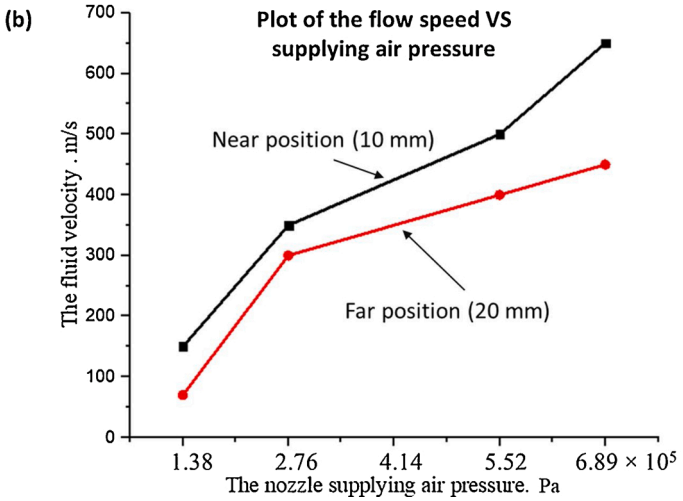

Fig. 5. Comparison of the fluid velocity at the tooltip at different distances and supplying air pressures of the nozzle outlet.

Fig. 10 shows the progression of average PCD tool flank wear with the increasing cutting distance at different air blowing pressure. The tool wear of the PCD tool land increases gradually for all 4 conditions. In particular, the tool's wearing rate becomes higher when the cutting distance is above 600 m for 1.38×10^5 Pa and 2.76×10^5 Pa conditions. In comparison, for 5.52×10^5 Pa supplying air pressure, the wearing rate has become even smaller, making the eventual tool wear land much smaller than the other conditions. It is interesting to find that 6.89×10^5 Pa supplying pressure does not give further reduced tool wear compared to 5.52×10^5 Pa. This could be caused by undesired tool-workpiece vibration due to the significantly large air-blowing pressure, and the reason for such phenomenon will be further discussed in the following sections based on the force and vibration analysis.

4.1. Results of surface roughness and cutting force

The surface roughness of the workpiece and the cutting force is also investigated for every 200 m cutting distance as well. A stylus profilometer has been used to evaluate the surface quality, using a stylus tip made of diamond with a 2 μm nose radius and 90 ° included angle. The cut-off length in calculating the roughness is set to be 80 μm for the roughness data processing. Fig. 11 shows the average surface roughness for the cutting distance for the tests with a near-positioned nozzle. As shown in Fig. 11, measured surface roughness has a similar but not identical progression trend with the tool flank wear, and 5.52×10^5 Pa supplying air pressure still leads to the lowest surface roughness compared to all the other 3 air-blowing conditions.

Generally, an increased tool flank wear will increase the amount of material elastic recovery more plowing, and less material shearing. Thus resulting in a less efficient material removal process. Larger tool-workpiece vibration and more unstable cutting force are also expected for a larger tool flank wear and may lead to larger surface roughness. However, increased plowing on the machined surface could pose a positive effect on the surface finish at a certain condition. A slightly worn cutting edge with ultrasonic vibration may create a lapping effect on the workpiece and eventually lower the height of vibration and feed

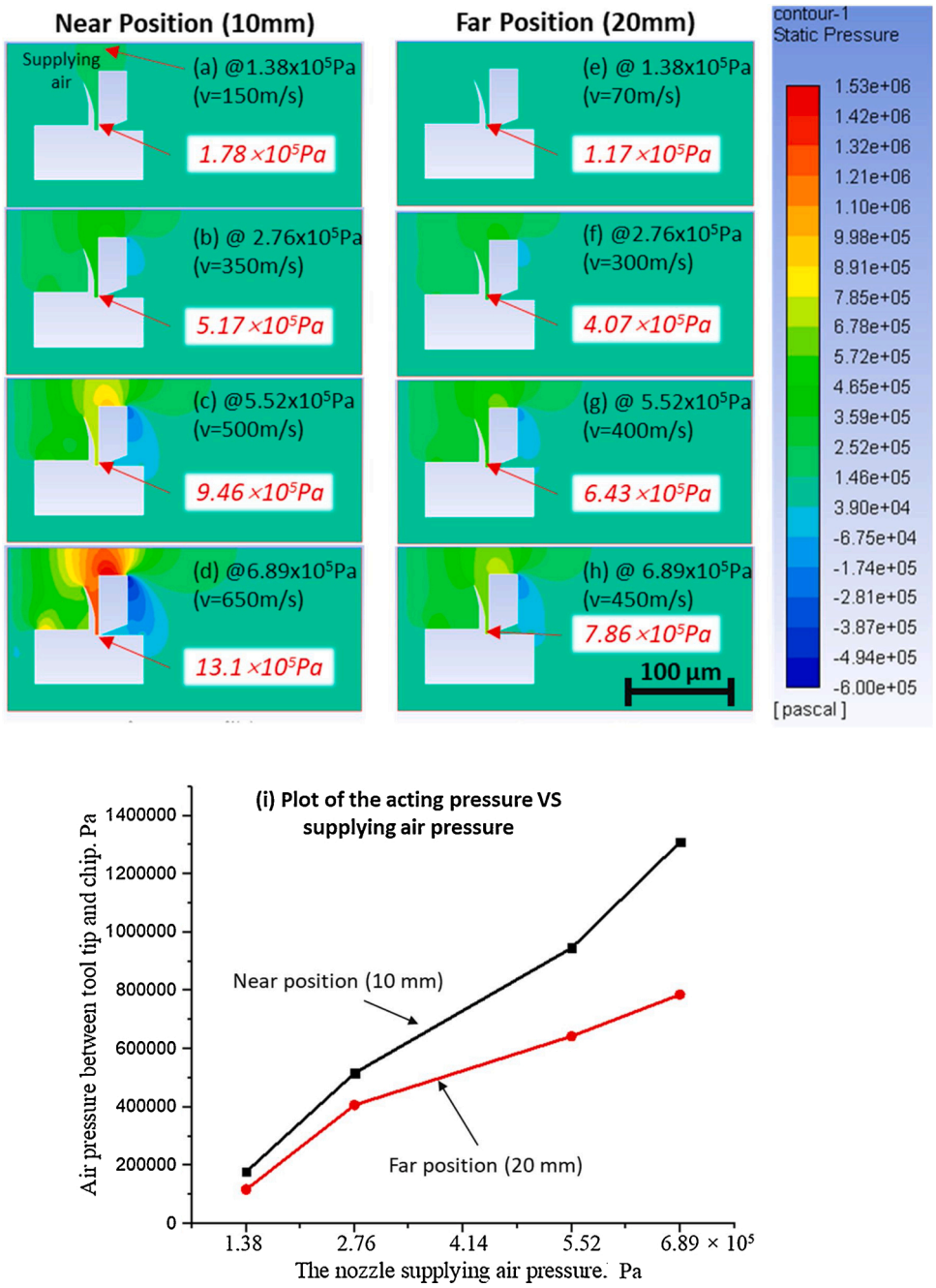

Fig. 6. Simulated acting air pressure at the cutting interface, with the nozzle at (a)-(d) near position, 10 mm and (e)-(h) far position, 20 mm. (i) The plot of the acting pressure at different supplying pressure.

marks. A typical example of this can be observed from the surface roughness variation of 5.52×10^5 Pa at the 2nd cutting round (i.e. 200 m–400 m). Although the tool wear land is increased from 6 µm to 11 µm, as shown in Fig. 10(b), the surface roughness (*Ra*) on hardened stainless steel has been found to improve with increasing acting air pressure.

The force in cutting and thrust directions during the machining process is monitored using a Kistler dynamometer (Type *9256C*), which sits below the ultrasonic vibrator and above the Z-axis, as shown in Fig. 12(a). The instant cutting force in the thrust direction is recorded at the beginning of each cutting round, i.e. when the cutting distance reaches 2 m, 202 m, 402 m, and 602 m. Fig. 12(a) and (b) show the measured thrust force at 602 m cutting distance for the 4 different air blowing pressure, as well as the variation of thrust-directional force with the increment of cutting distance, which is similar to the trend of tool wear progression as shown in Fig. 10(b).

Similar to the tool wear results in Figs. 9 and 10, it can be seen from Figs. 11 and 12 that the blow pressure of 6.89×10^5 Pa does not lead to better surface finish nor lower cutting force, which could be caused by the induced tiny impact or vibration of the tooltip due to the significantly large air blowing velocity. The resultant effect of the compromised system stability has exceeded the effect of the tool wear suppression from the sub-millisecond oxidation. To further explore the reason for such phenomenon, an additional test is conducted to record the force signal measured by the dynamometer at different air blowing pressure, but without any cutting activity. Fast-Fourier Transform (FFT) is conducted on the recorded force data to process the force signal from its original domain to a representation in the frequency domain. Fig. 13 (a) shows the FFT results for 3 air blowing pressures, and Fig. 13(b)

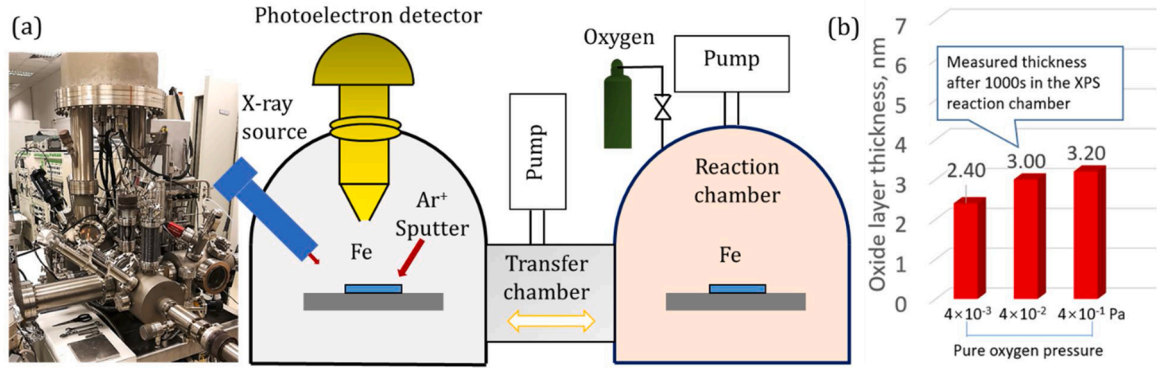

Fig. 7. (a) Photo and schematic of the XPS system used, (b) measured oxide thickness after 1000 s exposure under three different pure oxygen pressures.

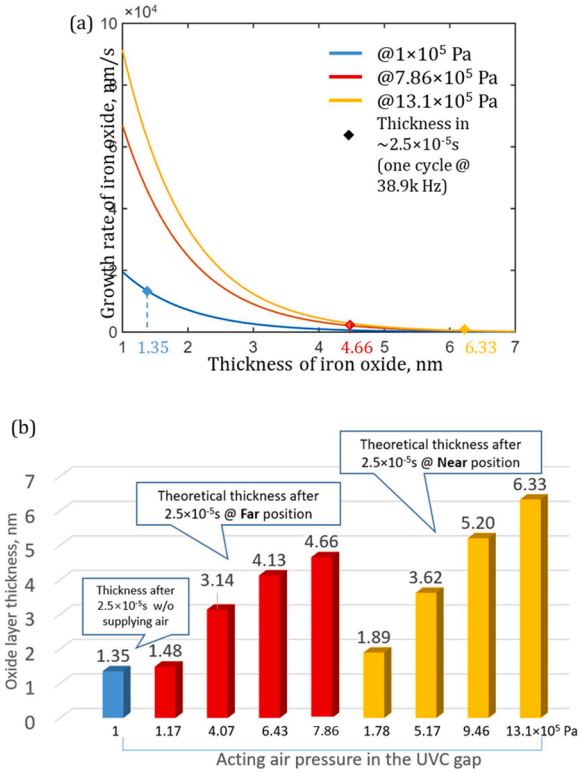

Fig. 8. (a) Calculated oxide growth rate at different acting air pressure and (b) the oxide thickness grown within one vibration cycle, i.e. 2.5 × 10^{-5} s.

Table 2
Oxide layer thickness within 1 UVC cycle time with different air pressures.

Nozzle position	Far Position (20 mm)				Near Position (10 mm)			
Supplying air pressure, 10^5 Pa	1.38	2.76	5.52	6.89	1.38	2.76	5.52	6.89
Acting air pressure around the cutting zone, 10^5 Pa	1.17	4.07	6.43	7.86	1.78	5.17	9.46	13.1
Calculated grown thickness of oxide, nm	1.48	3.14	4.13	4.66	1.89	3.62	5.20	6.33

draws the absolute amplitude value at 3 specified frequencies under different air blowing pressures. A peak value of the FFT-analyzed force amplitude at a certain frequency usually represents a vibration with a certain amplitude at such frequency, induced by the ultrasonic actuator or the blowing air.

It can be seen that, besides the ultrasonic frequency induced by the actuator (38.9 kHz), the amplitude at the other two frequencies (13.7 kHz and 19.9 kHz) has drastically increased when the air blowing pressure has reached 6.89 × 10^5 Pa, meaning that the tooltip vibration induced by the actuator has become unstable due to the surrounding high-velocity air blowing. The pressure applied around the ultrasonic vibration device and tool could induce a force along the direction of the air blow, thus causing the tool system to deform slightly. This passive deformation may fluctuate following the turbulence of the gas flow, causing external disturbance besides its controlled ultrasonic vibration. As the extent of deformation relies on the acting force, the system may become unstable with the increasing air blowing pressure. This will eventually cause non-consistent engagement and separation between the tooltip and the workpiece in terms of amplitude and frequency. Moreover, from Fig. 13(b), it can also be seen that the force amplitude at the frequency 38.9 kHz has slightly dropped at 6.89 × 10^5 Pa, possibly caused by a smaller vibration amplitude due to the high air blowing pressure. The smaller amplitude may eventually lead to a smaller vibration gap between the tool and the workpiece and hence affect the diamond tool wear suppression in UVC.

4.2. Experimental investigation using single crystal diamond tools

PCD is a type of composite material, in which fine-grain diamond particles are bound with cobalt alloy by sintering them together at high temperature and high pressure. Although the diamond particles usually have a weight percentage of around 90 %, their wear mechanism may still be different from a single crystal diamond (SCD), in which there is no metal binder material and the binding strength between neighboring carbon atoms is stronger due to its three-dimensional sp3 structure. Normal PCD tools usually have a lower hardness and a higher toughness than SCD tools, and the wearing rate for PCD tools is usually higher than SCD tools, except the binderless nano-polycrystalline diamond tools proposed by Harano et al. (2012).

As SCD tools usually have better cutting performance due to the sharper cutting edge (radius ≤ 0.05 μm) than PCD tools (edge radius ≥ 5 μm), they are utilized in the machining of various optical components to obtain a better surface finish, profile accuracy, and higher dimensional stability. To investigate the impact of coolant air blowing pressure on the tool wear progression of SCD tools, another set of experiments is conducted to cut the same workpiece using 2 SCD tools with 0.2 mm nose radius under 2 different air blowing pressure, i.e. 1.38 × 10^5 Pa and 5.52 × 10^5 Pa. It has been reported by Shamoto and Moriwaki (1999) that, with the assistance of ultrasonic vibration, the tool life for SCD can

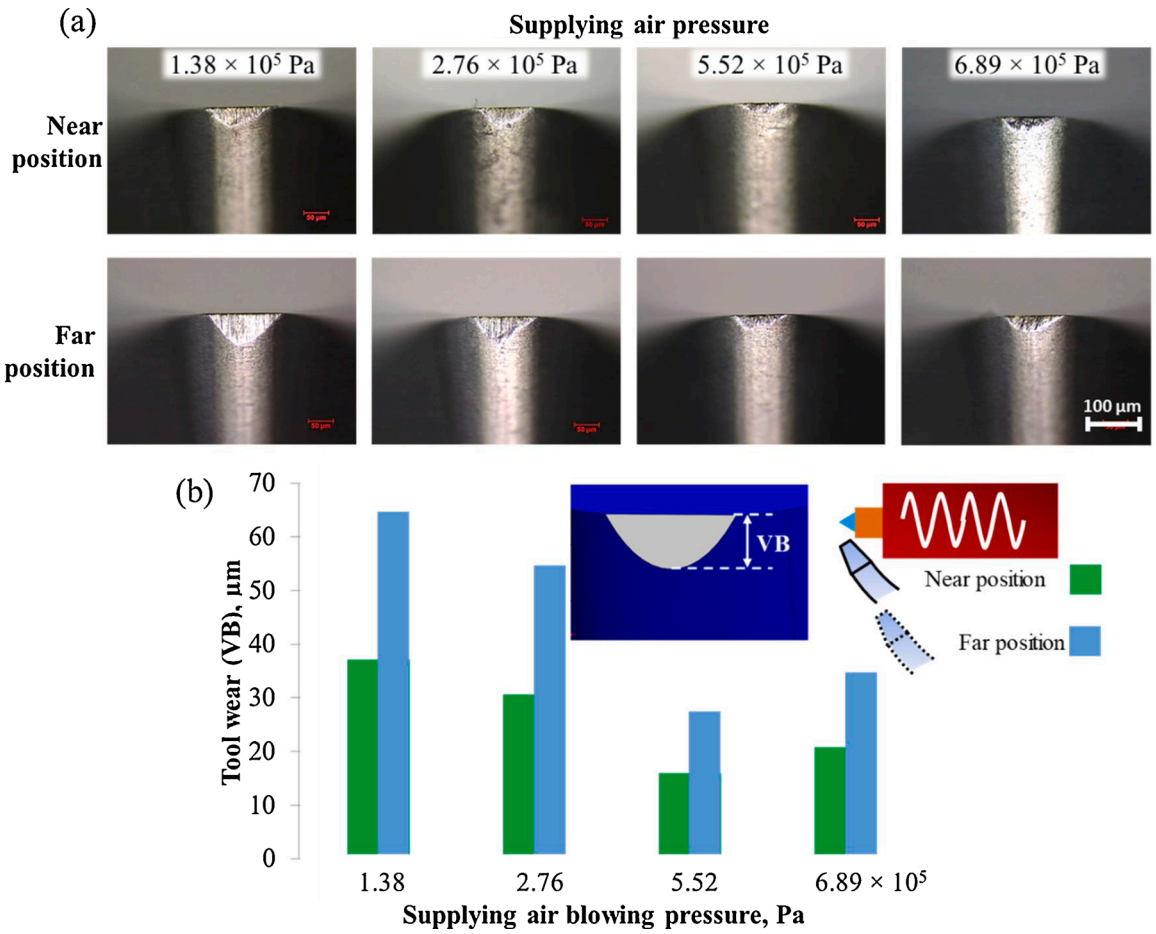

Fig. 9. (a) Microscopic images of PCD tool flank faces for different supplying air blowing conditions, and (b) tool flank wear for different supplying air blowing pressures.

last for 2 km or more. Hence, in the study, to shorten the machining time and accelerate the tool wear, instead of applying a low cutting speed as in the PCD test (20 RPM), the spindle speed is set at a relatively higher value (40 RPM), because it has already been observed that the increment of cutting speed in UVC will drastically increase the tool wear by a few times, as reported by Zhang et al. (2014).

The SCD tools are taken out for measurement using a digital microscope and a scanning electron microscope (SEM) after 400 m cutting distance, as shown in Fig. 14. It can be seen that the flank wear for 1.38 $\times$ 10^5 Pa supplying air pressure is 1.7 times that for 5.52 $\times$ 10^5 Pa. As a comparison, at 400 m cutting distance, the flank wear of PCD tool (close position) for 1.38 $\times$ 10^5 Pa is 1.2 $\times$ that for 5.52 $\times$ 10^5 Pa (see Fig. 10 (b)), meaning that increased supplying air pressure may have a larger effect on suppression of the flank wear for SCD tool. It could be caused by the more weight percentage of diamond in SCD tools than in PCD tools.

5. Discussion

Based on the observed experimental results above, it can be confirmed that air-blowing pressure has a significant impact on the wearing rate of diamond tools in UVC of steel for both PCD and SCD tools. An increased air blowing pressure will slow down the tool wear rate, the value of which depends on the type of diamond tools as well as the cutting conditions. As mentioned in Section 1, as the tool wear suppression mechanism for UVC of steel is still not clear until now, it is necessary to discuss the root cause for such phenomenon in this section. As the increased air blowing pressure does not pose any effect on the other cutting parameters, it should not affect the tool-workpiece contact time during UVC. Hence, this proposed hypothesis cannot explain the phenomenon observed in this study.

Instead, both the other two hypotheses could well explain the results obtained above. On one hand, an increased air blowing pressure will increase the air flowing speed around the cutting zone, and hence could provide enhanced cooling and take away more heat from the tool and the workpiece. As Brinksmeier and Gläbe (2002) have proven that a reduced environmental temperature will lower the chemical reaction rate between iron and carbon as well as the chemical tool wear rate of the diamond, it is possible that the increased air blowing pressure lead to the same result. On the other hand, an increased air blowing pressure applied around the cutting zone will also bring more air, thus more oxygen molecules, into the gap between the tooltip and the workpiece in each vibration cutting cycle. As there is 21 % oxygen in the environmental air, more oxygen molecules will get in contact with the freshly cut steel surface and could lead to a faster generation or a thicker layer of inert iron oxide on the surface to prevent the direct contact and chemical reaction between diamond and iron atoms when the tool touches the workpiece later. However, it is still difficult to identify which hypothesis is the true reason for the phenomenon observed in this study. Hence, the following section discusses it from several points of view.

5.1. Experiment on no air blowing to UVC process

According to the discussion above, it can be drawn that the observed phenomenon can be attributed to both hypotheses: lower cutting temperature and slower iron oxide generation due to the reduced air blowing pressure. Based on the experiments conducted in Sections 4.1 and 4.2, it is difficult to identify the exact reason for the observed

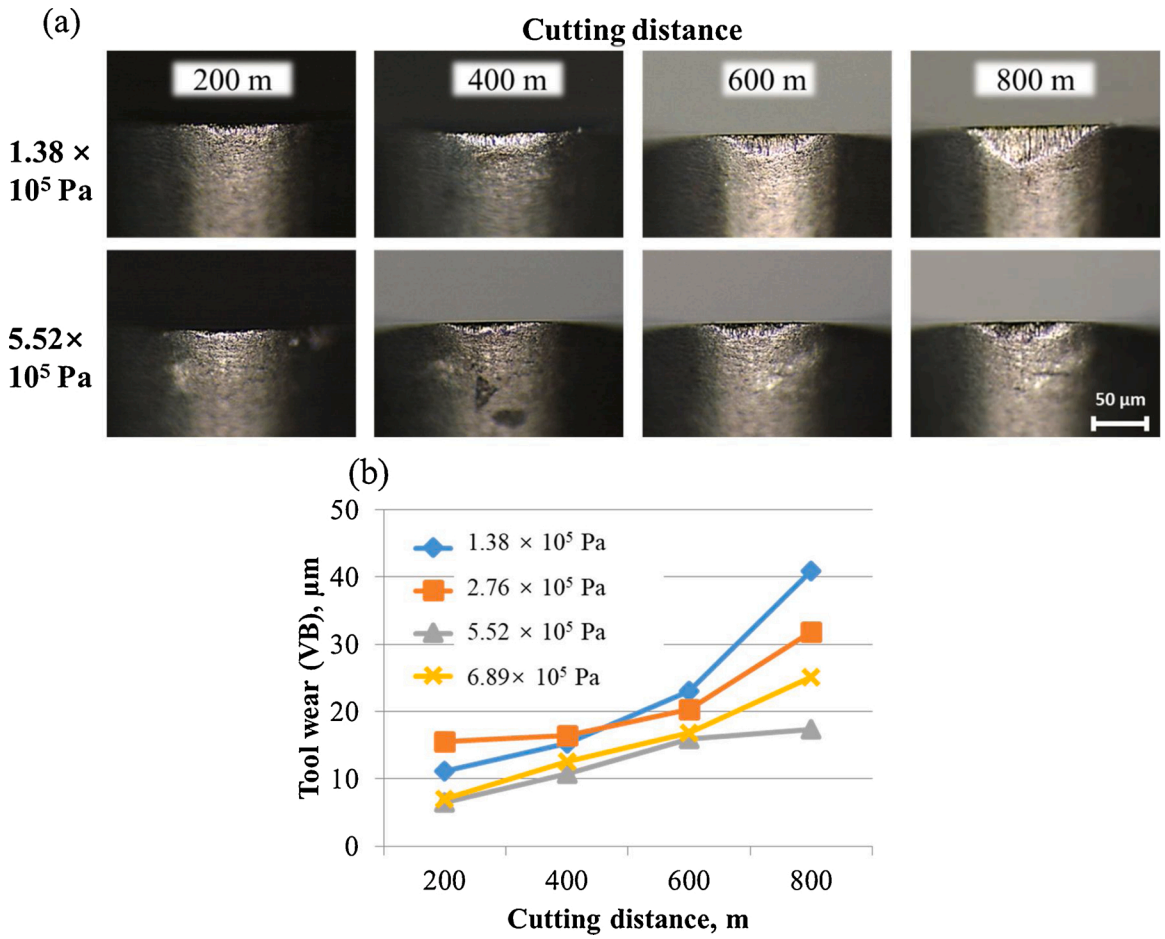

Fig. 10. (a) Microscopic images of PCD tool flank faces after different cutting distances, and (b) measured tool flank wear for different air blowing pressure and cutting distances when the nozzle is at the near position.

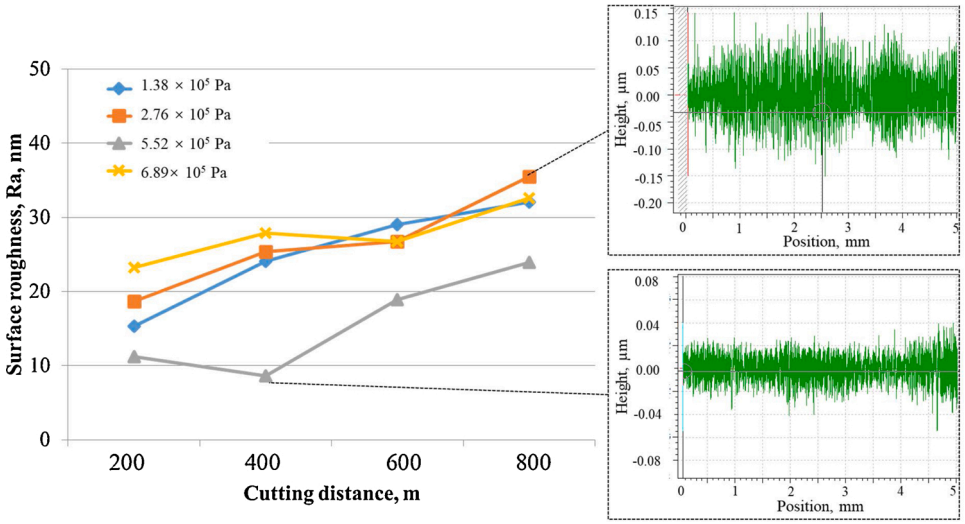

Fig. 11. Surface roughness with different cutting distances under different air-blowing pressure.

phenomenon. Hence, another set of experiments is conducted to study the tool wear progression with no coolant air blowing. However, if the tool rake face is still facing upward, due to the gravity and no blowing air, the generated chips will stack on top of the tool rake face if they are not blown away. The accumulated chips may affect the ultrasonic vibration induced by the horn as well as the intermittent cutting process. Therefore, for the experiment setup with no air blowing, the tool rake face is flipped to face downward to allow the generated chips to fall themselves, as shown in Fig. 15. For comparison, additional two sets of the experiment are also conducted with 1.38×10^5 Pa air blowing pressure and conventional cutting with the absence of tool vibration, with the same experimental setup and nozzle location.

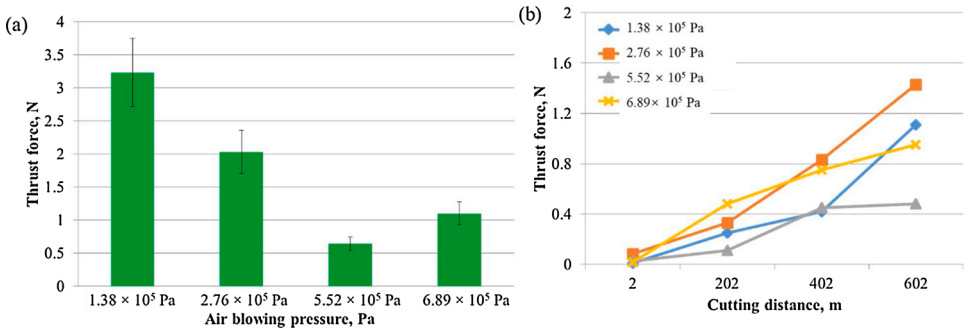

Fig. 12. (a) Averaged thrust directional cutting force under different air blowing pressure at 602 m cutting distance, and (b) measured thrust directional cutting force with the increasing cutting distance when the nozzle is at the near position (10 mm).

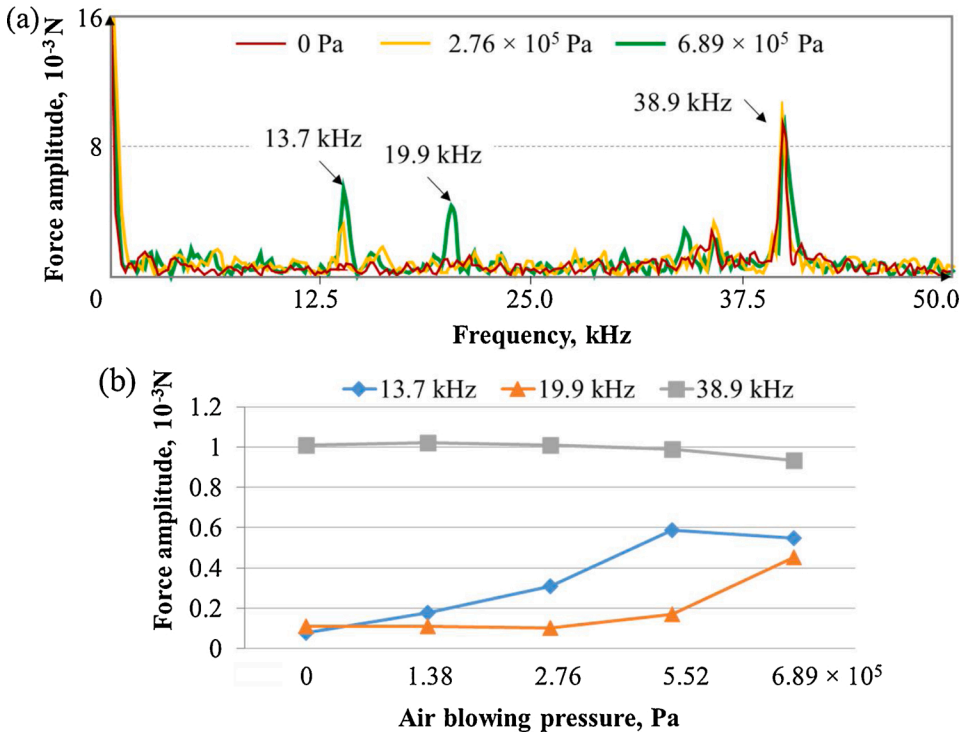

Fig. 13. (a) FFT analysis of measured thrust-directional force at 3 air blowing pressures with no cutting activity; and (b) variation of FFT-analyzed force amplitude at 3 specified frequencies.

Fig. 16 compares the tool wear results for the three tests. The tool wear with no air blowing is just slightly larger than the 1.38 × 10^5 Pa pressure air blowing. For the experiment with no air blowing, it is considered that there should be little air flowing around the cutting zone, and heat exchange between the environmental air and the cutting zone could be neglected. From Fig. 16(b), it can be found that the flank wear of the PCD tool after UVC with no air blowing is significantly smaller than the one with conventional cutting.

5.2. Proposed tool wear suppression mechanism of UVC

When a freshly cut steel surface is exposed to air or any gas containing oxygen, the oxygen is firstly absorbed onto the metal surface through a place-exchange reaction to form an initial monolayer of oxide, which should have a thickness of 0.3 nm (i.e. the spacing between Fe atoms of an Iron(II) Oxide lattice), as shown in Fig. 17. Once oxygen is absorbed, it is dissociated into chemisorbed atomic oxygen, which will then form covalent bonds with the metal atoms. Such covalent bonds will weaken the iron atoms' attachment to the surrounding metal lattice. Grosvenor et al. (2004) have calculated that only 5 ms is needed to form the first 0.3 nm oxide on steel surface under a low oxygen partial pressure of 1.3 Pa. By assuming that the growth rate of iron oxide is proportional to the oxygen pressure, it can be predicted that, under a standard atmospheric pressure (10^5 Pa), less than 20 μs is required for generating the first monolayer of oxide. In comparison, each vibration cutting cycle takes around 25 μs for the ultrasonic frequency (38.9 kHz) utilized in this study.

When oxidation continues, a new process will replace the place-exchange reaction, in which tunneling electrons from the metal will produce an electric field to the absorbed oxygen. Outward cation diffusion is responsible for the growth of Fe_3O_4, while anion diffusion is responsible for the growth of γ-Fe_2O_3, and this growth rate will be independent of the O_2 pressure. The oxide growth rate will decelerate exponentially over time because the electric field strength will be broken with the increment of oxide thickness. The work function also increases, impeding the travel of electrons to the metal surface and hence the oxide growth capability.

During the conventional cutting process, as the cutting edge

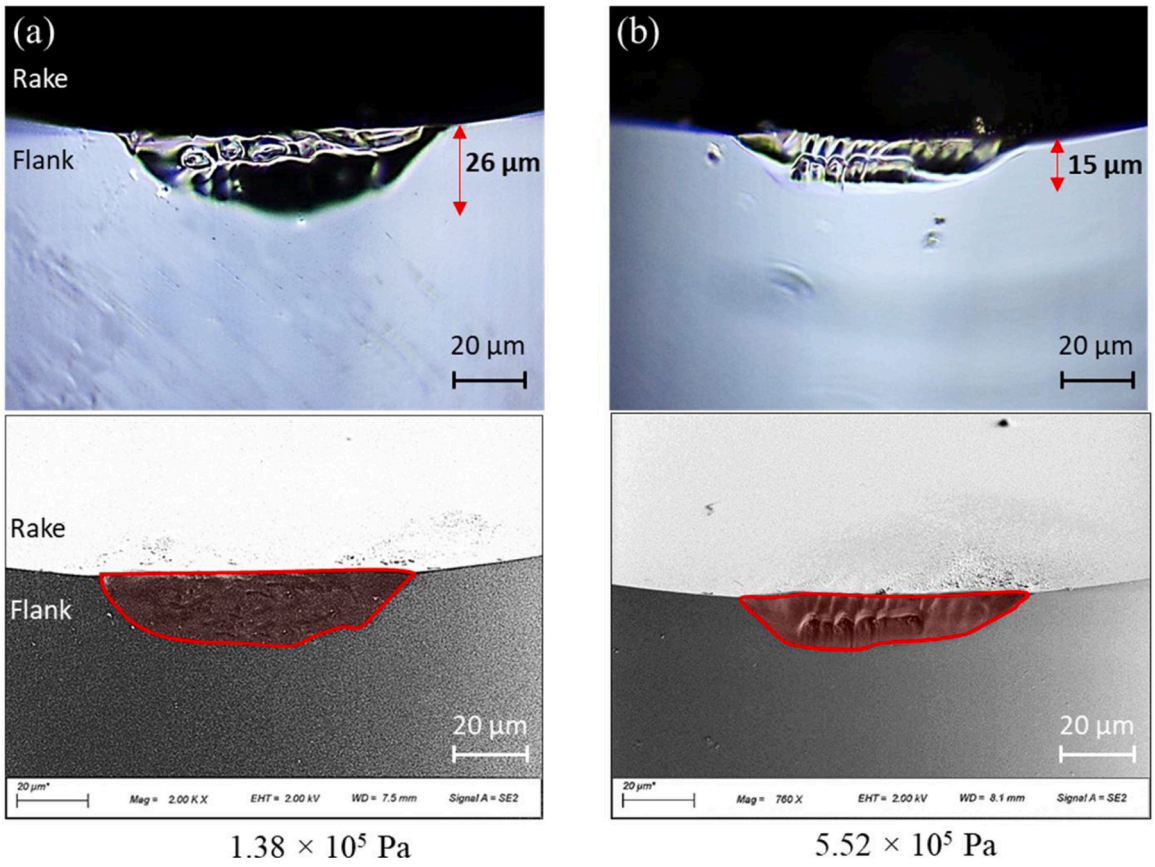

Fig. 14. A microscope and SEM pictures of the worn SCD tools after machining hardened stainless steel for 400 m under 2 air blowing pressures: (a) 1.38 × 10^5 Pa and (b) 5.52 × 105 Pa.

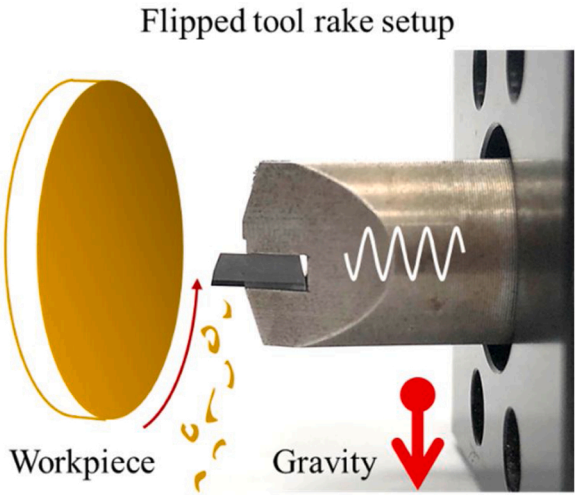

Fig. 15. PCD tool with flipped tool rake installed on the horn of the ultrasonic vibrator.

constantly contacts the cutting zone with no regular separation between the tool and the steel workpiece, a near-vacuum atmospheric condition is formed around the cutting zone, and the freshly cut workpiece will contact the diamond with no gap but the applied cutting force, as shown in Fig. 18(a). Such mechanical friction between the cutting edge and freshly cut iron atoms could strengthen the chemical wear between the diamond and the steel workpiece, resulting in catastrophic diamond tool wear in a very short cutting distance.

During the UVC process with normal air blowing pressure (20 PSI), a regular separation between the tool and the cutting zone occurs in an ultrasonic frequency, allowing the environmental air with 21 % oxygen to fill the gap and form an iron-oxygen covalent bond on the freshly cut steel surface, as shown in Fig. 18(b). From Section 3, it is understood that oxygen can be absorbed to form a monolayer of iron oxide in a very short time, which is comparable to the period of one vibration cycle. Although the formed oxide layer is thin, it could still able to work as a protective layer and could prevent chemical reactions between carbon and iron atoms to a certain extent. In the field of material science, it has already been fully understood about half a century ago by Bloom and Goldenberg (1965) that the active iron atoms can be passivated by forming a thin protective oxide film on the steel substrate.

During the UVC process with a higher air blowing pressure, more oxygen molecules will fill the gap above the cutting zone, resulting in more oxygen partial pressure above the freshly cut steel surface, as shown in Fig. 18(c). From Fromhold (1980), it is well known that an increased oxygen partial pressure can accelerate the formation of a thin iron oxide film on a metal substrate. More oxygen atoms absorbed on the steel surface could further passivate the active iron surface and weaken the chemical affinity between iron and carbon atoms. Moreover, it has also been observed by Wilson et al. (1980) that the formation of iron oxide on the steel substrate can reduce the friction coefficient in a high-vacuum condition until the complete oxide coverage is obtained because oxide-oxide contact has a much lower coefficient of sliding friction than metal-metal contacts. The generation of the oxide layer can also help to prevent tool wear by reducing the mechanical friction force as well the induced tribal-chemical reaction between diamond and iron atoms. Future work could be carried out to study this sub-millisecond oxidation behavior to quantitatively reveal the relationship between the UVC parameters and the tool wear, with the aid of X-Ray Diffraction (XRD) or Raman spectroscopy.

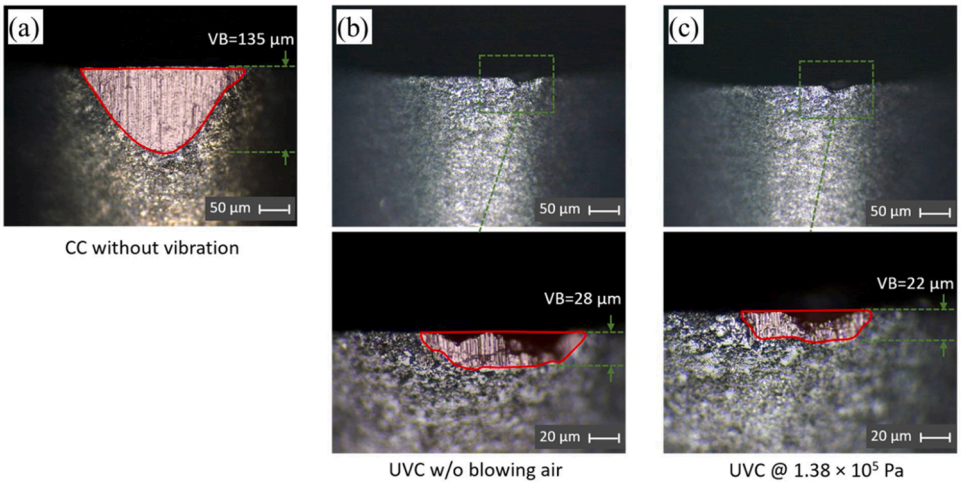

Fig. 16. Tool wear comparison between (a) conventional cutting without tool vibration, (b) UVC without blowing air, and (c) UVC with 1.38 × 10^5 Pa air blowing (Flipped tool setup; 300 m cutting distance for each test).

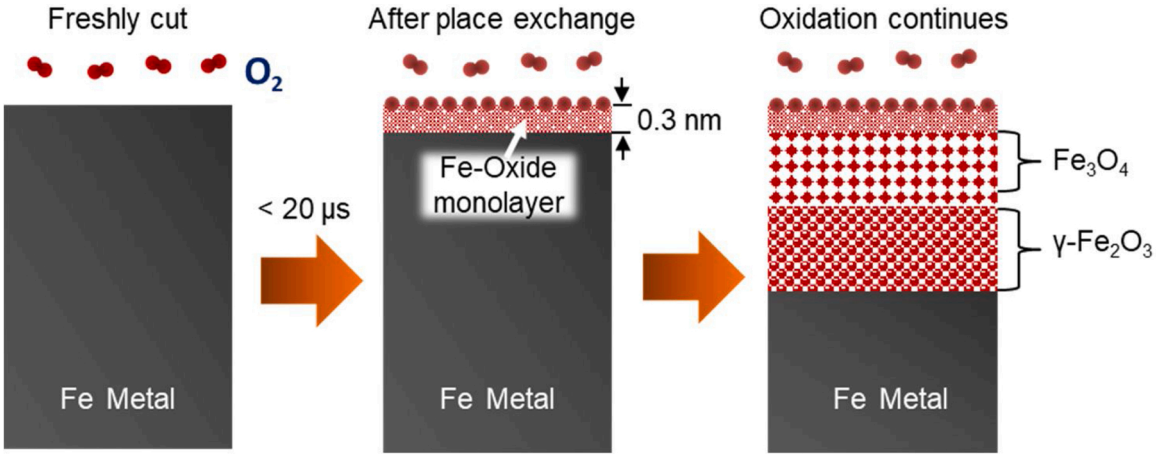

Fig. 17. Schematic steps for oxide growth on a freshly cut steel surface.

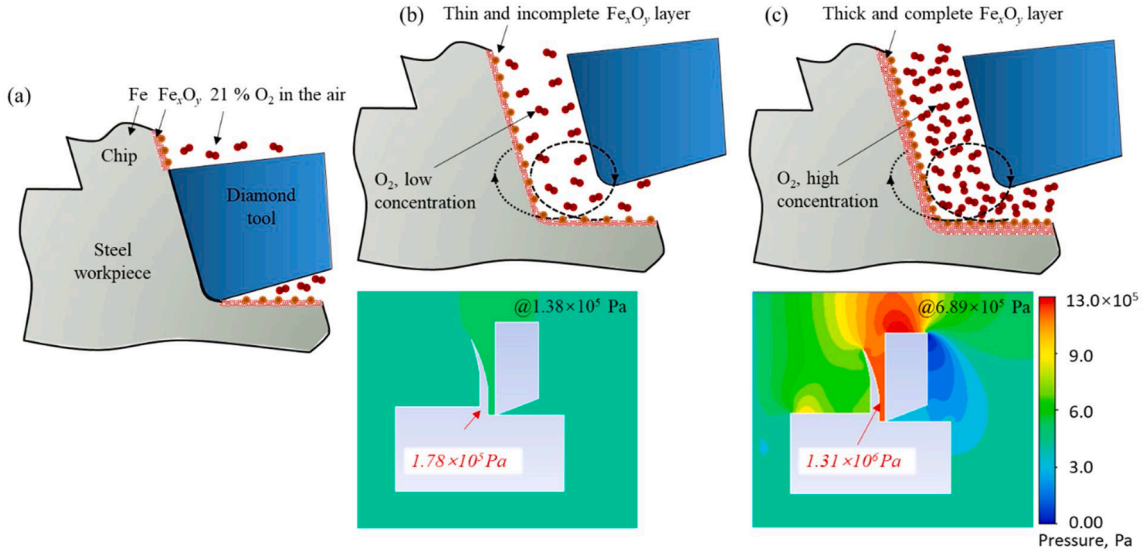

Fig. 18. Schematic illustration and CFD simulation of the iron oxide generation under the conditions of (a) intimate contact between tool and workpiece; (b) UVC with normal air blowing pressure; and (c) UVC with high air blowing pressure.

6. Conclusions

In this paper, the impact of air-blowing pressure on diamond tool wear in ultrasonic vibration cutting (UVC) of steel is systematically investigated. Through the results of UVC cutting tests on stainless steel using both polycrystalline diamond and single-crystal diamond tools, it can be concluded that larger relative air pressure within the cutting zone could suppress the tool wear of diamond, provided that the actuator-induced ultrasonic vibration is not affected by the high air blowing velocity. Such phenomenon is explained by the proposed tool wear suppression mechanism together with computational fluid dynamics (CFD) simulation on air flowing around the vibration gap in UVC. The following conclusions can be drawn:

1) CFD simulation of airflow has shown that an increased air blowing pressure will increase the instantaneous air pressure and density at the vibration gap around the cutting zone.
2) Increased acting air pressure at the tool-work interface will lead to a smaller wear rate for both polycrystalline diamond and single-crystal diamond tools.
3) An abnormally high air blowing pressure (6.89×10^5 Pa in this study) will adversely worsen the diamond tool wear compared to milder pressures, due to the disturbed and attenuated ultrasonic vibration resulting from the strong airflow and acting thrust force.
4) UVC with no air blown towards the cutting zone will still lead to a strong tool wear suppression effect compared to the conventional cutting, and can effectively reduce the diamond tool wear.
5) The conventional hypothesis of reduced tool-workpiece contact time and enhanced cooling cannot reasonably explain the experimental phenomenon observed in this study.
6) The preliminary calculation has shown that the sub-millisecond UVC interval is sufficient to form multiple oxide layers on freshly cut steel in a standard atmosphere, the oxide is thicker and more complete when the partial pressure of oxygen increases.

CRediT authorship contribution statement

Xinquan Zhang: Conceptualization, Methodology, Writing - original draft. **Rui Huang:** Conceptualization, Validation, Software, Writing - original draft, Supervision. **Yang Wang:** Formal analysis. **Kui Liu:** Project administration, Supervision. **Hui Deng:** Conceptualization, Methodology. **Dennis Wee Keong Neo:** Writing - review & editing, Resources.

Declaration of Competing Interest

The authors report no declarations of interest.

Acknowledgements

Funding: This work was financially supported by National Natural Science Foundation (52075332); Shanghai Pujiang Program (19PJ1404500); and A*STAR AME 1st Singapore-Germany Academic-Industry (2 + 2) International Collaboration Grant (A1890b0048).

References

Bloom, M., Goldenberg, L., 1965. γ-Fe2O3 and the passivity of iron. Corros. Sci. 5, 623–630.
Brehl, D., Dow, T., 2008. Review of vibration-assisted machining. Precis. Eng. 32, 153–172.
Brinksmeier, E., Gläbe, R., 2002. Precision machining of steel with ultrasonically driven chilled diamond tools. Proceedings of ASPE 2002 Annual Meeting, ASPE, p. 257.
Brinksmeier, E., Gläbe, R., Osmer, J., 2006. Ultra-precision diamond cutting of steel molds. CIRP Ann. 55, 551–554.
Clarke, C., Carswell, B., Carswell, R., 2007. Principles of Astrophysical Fluid Dynamics. Cambridge University Press.
Cong, W., Pei, Z.J., Deines, T.W., Treadwell, C., 2011. Rotary ultrasonic machining of CFRP using cold air as coolant: feasible regions. J. Reinf. Plast. Compos. 30, 899–906.
Eley, D.D., Wilkinson, P., 1960. Adsorption and oxide formation on aluminium films. Proc. R. Soc. Lond. A Math. Phys. Sci. 254, 327–342.
Fromhold Jr., A., 1980. Theory of Metal Oxidation, vol. 2.
Fukumori, S., Itoigawa, F., Maegawa, S., Nakamura, T., Shamoto, E., 2019. Suppression mechanism of diamond tool wear in ultrasonic vibration cutting. In: AIP Conference Proceedings, Vol. 2113.
Grosvenor, A., Kobe, B., McIntyre, N., 2004. Examination of the oxidation of iron by oxygen using X-ray photoelectron spectroscopy and QUASESTM. Surf. Sci. 565, 151–162.
Harano, K., Satoh, T., Sumiya, H., 2012. Cutting performance of nano-polycrystalline diamond. Diam. Relat. Mater. 24, 78–82.
Moriwaki, T., Shamoto, E., 1991. Ultraprecision diamond turning of stainless steel by applying ultrasonic vibration. CIRP Ann. 40, 559–562.
Paul, E., Evans, C.J., Mangamelli, A., McGlauflin, M.L., Polvani, R.S., 1996. Chemical aspects of tool wear in single point diamond turning. Precis. Eng. 18, 4–19.
Shamoto, E., Moriwaki, T., 1994. Study on elliptical vibration cutting. CIRP Ann. 43, 35–38.
Shamoto, E., Moriwaki, T., 1999. Ultaprecision diamond cutting of hardened steel by applying elliptical vibration cutting. CIRP Ann. 48, 441–444.
Suzuki, N., Haritani, M., Yang, J.B., Hino, R., Shamoto, E., 2007. Elliptical vibration cutting of tungsten alloy molds for optical glass parts. CIRP Ann. 56, 127–130.
Wilson, J., Stott, F., Wood, G.C., 1980. The development of wear-protective oxides and their influence on sliding friction. Proc. R. Soc. Lond. A Math. Phys. Sci. 369, 557–574.
Zhang, X., Liu, K., Kumar, A.S., Rahman, M., 2014. A study of the diamond tool wear suppression mechanism in vibration-assisted machining of steel. J. Mater. Process. Technol. 214, 496–506.
Zhang, X., Deng, H., Liu, K., 2019. Oxygen-shielded ultrasonic vibration cutting to suppress the chemical wear of diamond tools. CIRP Ann. 68, 69–72.